Posttraumatic osteonecrosis in a swine model

Correlation of blood cell flux, MRI and histology

John Gray Seiler, III[1], Philip J Kregor[2], Ernest U Conrad, III[3] and Marc F Swiontkowski[3]

We used a miniature swine femoral neck fracture model to demonstrate the effects of the fracture on blood flow, histologic appearance, MRI signal and the development of posttraumatic osteonecrosis. The fracture was created and internally fixed in the right hip of 11 swine, with the left hip serving as the control. Femoral head blood flow via Laser Doppler Flowmetry and MRI data was examined for the experimental hip preoperatively, postoperatively and at 1, 2, 4 and 8 weeks postfracture. At 8 weeks, the animals were killed and the femoral heads were evaluated. Femoral head blood flow decreased immediately postfracture and continued to diminish with time. MRI signal intensities in the femoral head at 4 and 8 weeks were significantly less when the fixation failed than when it was intact. Histologic grades (0–14 points) and bone densities were 7.6 and 49%, respectively, on the experimental side, compared to 1.6 and 56% on the control side. Histologic grading, bone density values and blood flow data had no relation to changes in MRI signal intensity.

Departments of Orthopedics, [1]Emory University, 1365 Clifton Road Atlanta, GA 30322, USA; [2]University of Mississippi, 2500 N. State St., Jackson, MS 39216, USA; [3]University of Washington, Harborview Medical Center, Seattle, WA, USA. Correspondence: Dr. Marc F Swiontkowski, Department of Orthopedics, Harborview Medical Center, 325 Ninth Avenue, ZA-48, Seattle, WA 98104, USA. Tel +1 206 731-5414. Fax -3227
Submitted 95-05-02. Accepted 96-01-25

Magnetic resonance imaging (MRI) is the diagnostic modality that is most useful for the early detection of femoral head osteonecrosis, and the nature of signal intensity deterioration in osteonecrosis is well-described (Genez et al. 1988, Hauzeur et al. 1989, Robinson et al. 1989). However, a negative MR does not exclude the diagnosis of osteonecrosis (Genez et al. 1988). In the setting of acute trauma, there is little information regarding the interval of time in which the MRI can reliably show changes consistent with osteonecrosis. We correlated the time sequence of MRI changes to changes in femoral head blood flow and ultimate appearance of the femoral heads in a miniature swine model of posttraumatic proximal femoral osteonecrosis.

Animals and methods

Initial surgery: femoral neck fracture, fixation, and Doppler readings

After obtaining baseline magnetic resonance images under ketamine sedation, as described below, 12 40–60 kg skeletally mature (age 14–20 months) Gottinger miniature swine were sedated with an intramuscular injection of ketamine and orotracheally intubated. Satisfactory general anesthesia was maintained with a mixture of 1.0% halothane and 100% oxygen. A posterolateral approach was made to the right hip of all animals. The left hip was used as a control. A 5.0 mm hollow aluminum screw with a teflon coating and plastic sleeve assembly was inserted into the posterior wall of the acetabulum. Aluminum was used as the material for the screw to prevent distortion of the MRI signal. The screw was oriented under direct vision towards the superior and lateral portion of the femoral head (Figure 1). The femoral head blood cell flux (BCF) was measured through the hollow screw and sleeve assembly with a 2.2 mm flexible laser Doppler flowmetry (LDF) probe (Periflux Pf2, 114 86 Stockholm, Sweden). All LDF readings were averaged over 6 seconds, and stored on a digital storage oscilloscope (Model 4094, Nicolet Instrument Corp., Madison, WI 53711, USA). A basilar femoral neck osteotomy (simulating a fracture) was then created with a 1.5 mm osteotome and the BCF was again measured. The fracture was reduced under direct vision and internally fixed with two 1.6 mm commercially pure titanium Kirschner wires. This material was chosen to eliminate MRI artifact. The BCF was again measured after internal fixation.

Animal groups

1 animal died perioperatively from the anesthetic.

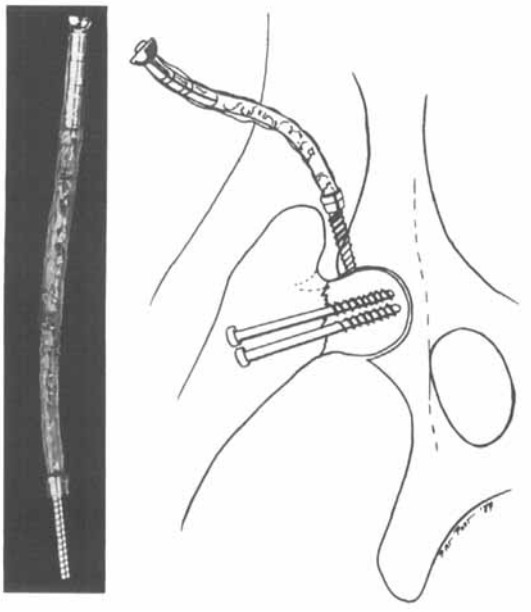

Figure 1. Placement of hollow aluminum screw with plastic sleeve assembly in the posterior wall of the acetabulum. This allowed the laser Doppler flowmetry probe to be inserted through the acetabulum. Plastic sleeve assembly with hollow aluminum screw attached.

This left 11 swine available for study. 2 of these animals developed significant wound complications which necessitated killing after collection of the 1 week data. 7 animals had some degree of failure of their internal fixation with loss of anatomic reduction by the 1 week interval, which was documented on MRI and was confirmed visually at the time of final exploration. In 4 animals, the fixation remained intact throughout the experiment and this group was analyzed separately.

Doppler measurements

Repeat femoral head BCF values were obtained under ketamine sedation at 1-week, 2-week, 4-week and 8-week intervals. At the time of the index operation, the end of the screw and sheath assembly were placed in subcutaneous tissue to permit later access for percutaneous Doppler assessment. In a subsequent procedure, a small incision was made and the sheath was identified. After irrigating the sheath with normal saline to clean debris, the flexible Doppler probe was placed through the sheath and hollow screw to impact on the femoral head. Placement was confirmed in most cases by the presence of a pulsatile blood cell flux. Doppler measurements were then obtained and recorded as previously described. In the interval between operations, all animals were given food and water ad libitum and were allowed weight bearing so far as tolerated.

MRI

All magnetic resonance images were obtained on a 1.5 Tesla imager (Siemens Magnetom 63, Siemens Medical Systems, Inc., 186 Wood Ave. South, Iselin, NJ 08830, USA). T_1-weighted images were obtained at 4.0 mm intervals throughout the coronal plane of the femoral head with a T_R = 0.60 milliseconds and T_E = 15 milliseconds. Standard window contrast settings (W = 1060, C = 400) were used to print each slice. Images were obtained as a baseline, immediately postoperatively and at 1-week, 2-week, 4-week and 8-week intervals. T_1 MRI intensity values for a given hip were expressed as a ratio of the femoral head intensity in the superolateral aspect of the femoral head divided by the intensity seen in the intertrochanteric region in the control femur. MRI intensity ratios were expressed as the ratio of the intensity value of the experimental hip divided by the intensity value for the control side.

Macro- and microanalyses of the femoral head

5 minutes prior to killing the animals with a barbiturate overdose, 62 mg/kg of 4% disulfine blue was intravenously administered for later quantification of vascularization of the femoral head. The right and left femora were then explanted and immediately stored at –70 °C. Plain radiographs of all explanted femora were obtained. The femoral heads were sectioned and examined by light and fluoroscopic microscopy (Olympus microscope, BH-TU with reflected light fluorescence attachment, Shinjuku, Tokyo, Japan).

Bone density data were calculated by a video image analyzer (Scan Jet Plus Scanner, Hewlett-Packard, Inc.) linked to image processing software (Image 1.41, National Institute of Health, Bethesda, MD, USA) via a Macintosh computer (Model IIsi, Apple Computer Inc., Cupertino, CA, USA). With this, the trabecular bone surface area could be expressed as a percentage of a given view field in the superolateral aspect of the femoral head.

The femoral heads were sectioned and stained with standard hematoxylin and eosin. Histologic grading of the femoral heads was performed in a blind manner. The femoral head was divided into four quadrants above and two quadrants below the physeal scar. Each quadrant was then graded as having no (0), intermediate (1) or significant (2) involvement with each of the following 7 histologic parameters associated with osteonecrosis (Sevitt 1964, Catto 1965, Enneking 1977, Kenzora et al. 1978):

1. Empty osteocyte lacunae
2. Marrow invasion with mesenchymal cells

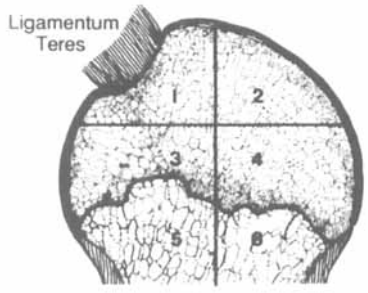

Table 1. Calculation of total histology score for each femoral head

Parameter	Zone						Total parameter score
	1	2	3	4	5	6	
1. Empty lacunae	A_1	A_2	A_3	A_4	A_5	A_6	$\Sigma A_n/6 = A$
2. Marrow invasion	B_1	B_2	B_3	B_4	B_5	B_6	$\Sigma B_n/6 = B$
3. Vascular ingrowth	C_1	C_2	C_3	C_4	C_5	C_6	$\Sigma C_n/6 = C$
4. Creeping substitution	D_1	D_2	D_3	D_4	D_5	D_6	$\Sigma D_n/6 = D$
5. Marrow fibrosis	E_1	E_2	E_3	E_4	E_5	E_6	$\Sigma E_n/6 = E$
6. Subchondral bone thinning	F_1	F_2	F_3	F_4	F_5	F_6	$\Sigma F_n/6 = F$
7. Chondral collapse	G_1	G_2	G_3	G_4	G_5	G_6	$\Sigma G_n/6 = G$

Each of 6 zones was evaluated and given a score of 0 (no), 1 (intermediate), or 2 (severe) for each of several histologic parameters. A total parameter score was calculated as the average of the 6 zones for each of the 7 parameters. The total histology score was then obtained by adding the total parameter score for all 7 parameters. Thus, a total score of 14 was obtainable, with 0 representing completely normal histology and 14 representing severe osteonecrosis.

Table 2. Laser Doppler blood cell flux (mV) versus time for all 11 experimental hips. Significant decreases in femoral head blood cell flux were evident at weeks 1, 4, and 8 when compared with baseline. Mean *SE*

	Blood cell flux (mV)	
Baseline	1490	*465*
Fracture	869	*211*
ORIF	1123	*449*
Week 1	271	*77*
2	294	*94*
4	439	*158*
8	262	*83*

3. Vascular ingrowth / hypertrophy
4. Creeping substitution
5. Marrow fibrosis
6. Decrease in subchondral bone thickness, and
7. Chondral collapse

A total osteonecrosis score of 14 points was obtainable, with higher scores representing a more extensive degree of femoral head osteonecrosis (Table 1).

Statistics

Values for each group are reported as means with standard errors. LDF and MRI values for all 11 pigs at varying periods were analyzed with a paired (i.e., for the same animal) two-tail t-test, which presumes a normal distribution (parametric analysis). Osteonecrosis grades and porosity data between control and experimental hips were analyzed in a similar manner. In comparing LDF, MRI, and histologic data between the FI and FF groups, because of the small sample size (n 4 and 7), the Wilcoxon-Mann-Whitney rank sum test was utilized as a nonparametric test for the two independent groups. Statistical significance is reported with the respective p-value.

Results

At the time of explantation, 1 femoral head had significant external changes of cartilage softening and early collapse. Plain radiographs did not show a crescent sign in any of the experimental femora.

Femoral head blood cell flux

Significant inter-animal variation in femoral head blood cell flux, as assessed by Doppler, was seen. Blood cell flux values for all experimental hips are presented in Table 2. Baseline values of mean 1490 (SD 465) mV were obtained. After the animals sustained a femoral neck fracture, this value decreased to 869 (211) mV ($p > 0.05$ when compared to baseline). Significant decreases in femoral head blood cell flux were seen at weeks 1, 4, and 8. At week 8, BCF averaged 262 (83) mV ($p < 0.05$ when compared with baseline at weeks 1, 4, and 8).

In comparing the FI and FF groups, a trend towards increased blood cell flux was noted in the FI group (Table 3). This was significant only at week 4 ($p < 0.05$).

MRI

Magnetic resonance imaging intensity values for all 11 animals are seen in Table 4. A decrease in intensity was present in all periods after the fracture which was significant immediately after the fracture and at weeks 1 and 8. These data may be presented in a slightly different fashion. The MRI intensity ratio rep-

Table 3. Laser Doppler blood cell flux (mV) versus time for the fixation-intact (FI, n 4) and fixation-failed (FF, n 7) groups in the right experimental hip. There was a trend towards increased blood cell flux over time in the FI group as compared to the FF group, but this was not significant, except at week 4. Mean *SE*

Blood cell flux (mV)	FI group		FF group	
Baseline	1038	*186*	1750	*726*
Fracture	740	*222*	955	*333*
ORIF	1900	*1331*	735	*197*
Week 1	415	*160*	158	*75*
2	328	*199*	268	*89*
4	595	*302*	226	*94*
8	370	*175*	126	*44*

Table 4. MRI intensity values in all 11 animals. In comparing values from the experimental hip versus the control hip, significant differences were seen after the fracture (ORIF) and at weeks 1 and 8. Mean *SE*

MRI intensity	Experimental hip		Control hip	
Baseline	0.44	*0.02*	0.42	*0.02*
ORIF	0.39	*0.02*	0.44	*0.02*
Week 1	0.37	*0.02*	0.46	*0.02*
2	0.41	*0.02*	0.44	*0.02*
4	0.38	*0.03*	0.44	*0.02*
8	0.34	*0.04*	0.48	*0.03*

Table 5. MRI intensity ratios (experimental/control hip) in all 11 animals. The baseline ratio decreased immediately after fracture production and fixation ($p < 0.02$). This value decreased further at 8 weeks ($p < 0.02$ compared with immediate postfracture values). Mean *SE*

	MRI intensity ratio	
Baseline	1.08	*–0.07*
ORIF	0.90	*–0.04*
Week 1	0.82	*–0.04*
2	0.94	*–0.06*
4	0.88	*–0.07*
8	0.72	*–0.07*

Table 6. MRI intensity ratio versus time for the fixation-intact (FI, n 4) and fixation-failure (FF, n 7) groups. At weeks 4 and 8, the difference between the fixation intact group (FI, n 4) compared with the fixation failure (FF, n 7) group was significant ($p \leq 0.02$). Mean *SE*

MRI intensity	FI group		FF group	
Baseline	1.15	*–0.15*	1.03	*–0.06*
ORIF	0.89	*–0.06*	0.91	*–0.06*
Week 1	0.84	*–0.01*	0.81	*–0.05*
2	1.03	*–0.06*	0.86	*–0.08*
4	1.07	*–0.06*	0.71	*–0.06*
8	0.88	*–0.06*	0.60	*–0.08*

resents the ratio of the experimental to the control hip. These figures are seen in Table 5. A baseline ratio of 1.08 (0.07) decreased to 0.90 (0.04) immediately after fracture production with fixation ($p < 0.02$). This decrease continued until week 8, at which time the ratio averaged 0.72 (0.07) ($p < 0.01$ when compared with baseline). Representative MRI scans of a control and experimental hip are shown in Figure 2.

The MRI intensity ratio values were also compared between the FI and FF groups, as seen in Table 6. Statistically higher ratios were seen in the intact fixation group (FI), when compared to the failed fixation group (FF) at weeks 4 and 8.

Histologic analysis

Osteonecrosis histology grades averaged 7.6 (0.8) on the experimental side and 1.6 (0.4) on the control side ($p < 0.01$). Representative histological examples are seen in Figures 3 and 4. The range of the histology grades was 0.0–4.5 for the control hip and 4.3–11.2 for the experimental hip. There was no statistical difference between the FI (6.5 (1.0) and FF (8.4 (1.0)) groups as regards histology grades. The difference between the experimental and control femoral head osteonecrosis scores was also calculated for each animal. This value averaged 3.6 (1.5) in the FI group, and 7.5 (1.1) in the FF group ($p < 0.03$).

Bone density of femoral heads

The mean bone density on the experimental side was 49% and on the control side 56% ($p < 0.01$).

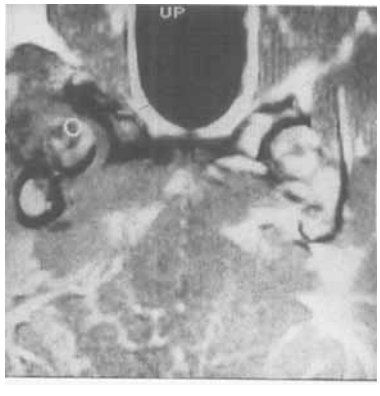

Figure 2. Representative MRI scan of control and experimental hips in a representative pig. The MRI intensity value for the right hip with significant osteonecrosis (both histologically and by MRI) was 0.28, while the contralateral hip had an intensity value of 0.47. This yields an MRI ratio of 0.6.

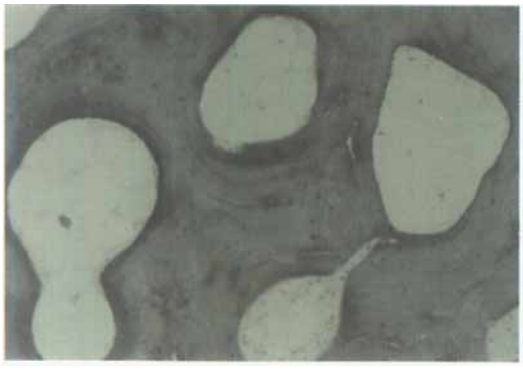

Figure 3. Histologic section of control femoral head showing no significant signs of osteonecrosis. Note viable of osteocytes and normal marrow fatty tissue.

Figure 4. Histologic section of experimental femoral head from same pig as shown in Figure 3. Definite osteonecrosis is exhibited by osteocyte dropout, mesenchymal cellular invasion, and marrow fibrosis.

Discussion

Previous work has utilized the technique of laser Doppler flowmetry to define the nature of regional blood cell flux changes in the proximal femur in patients with nontraumatic osteonecrosis (Swiontkowski et al. 1987, 1990). Patients evaluated at the time of core decompression were found to have a hypervascular region adjacent to the necrotic segment which had a decreased blood flow, as measured by laser Doppler flowmetry. These findings correlated well with previous histologic studies with femoral heads describing a remodeling front of bone adjacent to the necrotic area (Sevitt 1964, Catto 1965, Enneking 1977, Kenzora et al. 1978).

The T_1-weighted MR images in this study were significantly different from baseline immediately after fixation of the femoral neck fracture and throughout the experiment. Speer et al. (1990) found no significant change in MR images up to 48 hours in patients with femoral neck fractures. Additional research efforts may devise a better protocol for the earlier MRI detection of osteonecrosis following femoral neck fracture. Earlier detection of the osteonecrosis may be possible with the utilization of different spin-echo sequences or the addition of gadolinium contrast (Bloem et al. 1990). Using a rabbit femoral explant model, Lang et al. (1989) showed a significant change in T_1 relaxation times within 12 hours after explantation of their femurs. However, they noted that by 72 hours, MRI T_1 relaxation times had returned to near-baseline values. In their study, T_2 relaxation times did not demonstrate significant changes during their 72-hour experimental period. We have demonstrated that, in this animal model, magnetic resonance images can detect changes after a femoral neck fracture. The histologic correlation of the immediate imaging changes is not known, since no histologic evaluation was performed immediately after fracture.

We found no significant correlation between the laser Doppler flowmetry evaluation of femoral head blood flow, the histologic grading of the femoral head and the MR images. Our Doppler protocol utilized only 1 point of measurement and used no highly controlled mechanism for reproducing this in each animal, although we attempted to reproduce the position of the limb in each measurement session. This study utilized a small sample of animals. This finding, coupled with the significant inter-animal variation in Doppler output, may account for the lack of significant change in blood cell flux. Moreover, the laser Doppler probe averages the blood cell flux in the femoral head to a depth of 3.5 mm only in that portion of the head to which it is applied (Nötzli et al. 1989). Therefore, by sampling a relatively small area of the femoral head, this technique may underrepresent the blood flow changes in deeper portions of the femoral head.

A decrease in femoral head blood cell flux after femoral neck fracture was documented, which is consistent with standard theories about the development of traumatic osteonecrosis. Comparing the fixation-intact group with the fixation-failure group, there was a trend towards greater revascularization of the femoral head in animals with stable internal fixation.

Osteonecrosis grades and mean bone density showed a significant decrease, comparing the experimental side and the control side. The blinded histologic grading process assigned equal weight to each of the 7 factors associated with the progression of osteonecrosis (Sevitt 1964, Catto 1965, Enneking 1977, Kenzora et al. 1978). It is difficult to assign a numerical cutoff for the histologic grading scale which defines osteonecrosis. However, it was noted that a his-

tology score higher than 8 was associated with a significant increase in each of the 7 parameters and probably defines severe osteonecrosis. Some degree of osteocyte loss or pyknosis was seen in all of the experimental femoral heads. However, this was not always severe in otherwise definite cases of osteonecrosis. Catto (1965) and Kenzora et al. (1978) commented on the temporal delay of osteocyte dropout in osteonecrosis. Utilization of a multi-factorial osteonecrosis grading system may refine the ability to define histologically the diagnosis and may ultimately offer information of prognostic significance. The results of this study show only that acute femoral neck fractures cause changes in the femoral head in this model that are consistent with osteonecrosis and that it does so reproducibly.

We observed failure of the internal fixation, with loss of the anatomic reduction at the 1-week interval in 7 of the 11 animals. The creation, reduction, and fixation of the femoral neck osteotomy were all performed under direct visualization. It therefore seems unlikely that the osteotomy and/or reduction and fixation were considerably different from case to case. In addition, the immediate postoperative MRI scans of all 11 animals confirmed an anatomic reduction and appropriate position of the Kirschner wires. We therefore believe that the failure of the fixation was largely due to the malleability of the pure titanium wires.

In animals treated with stable fixation, no significant difference between the experimental and control hip in the MR signal was seen at 4–8 weeks. However, these animals show histologic changes of ischemia in the femoral head at 8 weeks. The absence of MRI signal intensity deterioration may be due to more rapid repair and revascularization by the host which is facilitated by stable fixation. Conversely, the animals with failure of their fixation devices had loss or limitation of fracture contact and limited opportunity for revascularization and repair. In these animals, significant deterioration of the MR images was seen by the 4–8-week interval. This deterioration could be due to the initial femoral head perfusion disturbance caused by the osteotomy and/or the lack of stable femoral neck fixation. There was no significant difference in the histologic scores between the fixation-failed and fixation-intact groups. This may be due to the 8-week period of postfracture observation being too short for total revascularization to occur. A longer period of observation might reveal greater trabecular microfracture, collapse, and higher osteonecrosis histology grades in the fixation-failed group, as compared to the fixation-intact group.

Acknowledgements

This study was supported by the Orthopedic Research and Education Foundations' Sir John Charnley Career Development Award.

References

Bloem J L, Reiser M F, Vanel D. Magnetic resonance contrast agents in the evaluation of the musculoskeletal system. Magn Reson Q 1990; 6: 136-63.

Catto M. A histological study of avascular necrosis of the femoral head after transcervical fracture. J Bone Joint Surg (Br) 1965; 47: 749-76.

Enneking W. Clinical Musculoskeletal Pathology. Storter Printing, Gainesville, FL 1977; 131-51.

Genez B M, Wilson M R, Houk R W, Weiland F L, Unger H R, Shields N N, Pugh K S. Early osteonecrosis of the femoral head: Detection in high risk patients with MR imaging. Radiology 1988; 168: 521-4.

Hauzeur J P, Pasteels J L, Schoutens A, Hinsenkamp M, Appelboom T, Chochrad I, Perlmutter N. The diagnostic value of magnetic resonance imaging in non-traumatic osteonecrosis of the femoral head. J Bone Joint Surg (Am) 1989; 7: 641-9.

Kenzora J E, Steele R E, Yosipovitch Z H, Glimcher M J. Experimental osteonecrosis of the femoral head in adult rabbits. Clin Orthop 1978; 130: 8-46.

Lang P, Jergensen H E, Genant H K, Moseley M E, Shulte-Mönting J. Magnetic resonance imaging of the ischemic femoral head in pigs: Dependency of signal intensities and relaxation times on elapsed time. Clin Orthop 1989; 244: 272-80.

Nötzli H P, Swiontkowski M F, Thaxter S T, Carpenter G K, Wyatt R. Laser Doppler flowmetry for bone blood flow measurements: Helium-neon laser light attenuation and depth of perfusion assessment. J Orthop Res 1989; 7: 413-24.

Robinson H J, Hartleben P D, Lund G, Schreiman J. Evaluation of magnetic resonance imaging in the diagnosis of osteonecrosis of the femoral head. J Bone Joint Surg (Am) 1989; 71: 650-63.

Sevitt S. Avascular necrosis and revascularization of the femoral head after intracapsular fractures: a combined arteriographic and histological necropsy study. J Bone Joint Surg (Br) 1964; 46: 270-96.

Speer K P, Spritzer C E, Harrelson J M, Nunley J A. Magnetic resonance imaging of the femoral head after acute intracapsular fracture of the femoral neck. J Bone Joint Surg (Am) 1990; 72: 98-103.

Swiontkowski M F, Ganz R, Schlegel U, Perren S M. Laser Doppler flowmetry for clinical evaluation of femoral head osteonecrosis: Preliminary experience. Clin Orthop 1987; 218: 181-5.

Swiontkowski M F, Christie M J, Ganz R, Schlehr F. Intraoperative bone blood flow measurement in patients with femoral head osteonecrosis. In: Bone Circulation and Bone Necrosis (Eds. Arlet J, Mazieres B). Springer-Verlag, Berlin, West Germany 1990; 150-3.